

# Short-range anisotropic ferromagnetic correlations in the paramagnetic and antiferromagnetic phases of $\text{Gd}_5\text{Ge}_4$

Z. W. Ouyang

*Ames Laboratory of the US DOE, Iowa State University, Ames, Iowa 50011-3020, USA*

V. K. Pecharsky\* and K. A. Gschneidner, Jr.

*Ames Laboratory of the US DOE, Iowa State University, Ames, Iowa 50011-3020, USA**and Department of Materials Science and Engineering, Iowa State University, Ames, Iowa 50011-2300, USA*

D. L. Schlager and T. A. Lograsso

*Ames Laboratory of the US DOE, Iowa State University, Ames, Iowa 50011-3020, USA*

(Received 7 June 2006; revised manuscript received 27 July 2006; published 6 September 2006)

Signatures of short range anisotropic ferromagnetic correlations and ferromagnetic clustering, manifested as unusually large hysteresis and other anomalies of the low magnetic field dc magnetization and ac magnetic susceptibility, have been observed in both the antiferromagnetic and paramagnetic states of single crystal  $\text{Gd}_5\text{Ge}_4$ . Ferromagnetic correlations, which are most pronounced in a weak magnetic field applied along the  $b$  axis, are readily suppressed by fields exceeding  $\sim 5$  kOe and are believed to be related to a Griffiths-like phase that develops in  $\text{Gd}_5\text{Ge}_4$  below  $T_G \cong 240$  K.

DOI: 10.1103/PhysRevB.74.094404

PACS number(s): 75.30.Kz, 75.50.Ee, 75.50.Cc

## I. INTRODUCTION

Continuing advancements in design and characterization of increasingly complex magnetic materials often lead to a progressively better understanding of ideas articulated in the past. One example is the so-called Griffiths phase (GP)—a peculiar magnetic state in which magnetization fails to be an analytical function of the magnetic field,  $H$ , between  $T_C$  and  $T_G$  when  $H$  approaches zero, where  $T_C$  is the conventional long range ferromagnetic (FM) ordering temperature (Curie temperature) and  $T_G$  represents the onset of completely random magnetic interactions (true paramagnetism)—first predicted to occur in randomly diluted Ising ferromagnets.<sup>1</sup> Recently, various systems exhibiting GP-like behavior are receiving considerable attention.<sup>2-7</sup> The appearance of the Griffiths phase is usually associated with competing magnetic interactions leading to FM clustering, the origin of which may differ from one material to another. For example, short-range FM clustering in the magnetically disordered, apparently paramagnetic (PM) but actually GP-like state of  $\text{Tb}_5\text{Si}_2\text{Ge}_2$  (Ref. 7) was associated at the microscopic level with competing intra- and interlayer magnetic exchange interactions, and at the macroscopic scale, with stacking faults that promote cluster nucleation and arise from microtwinning<sup>8</sup> which is found in all members of the extended series of  $R_5\text{Si}_x\text{Ge}_{4-x}$  compounds ( $R$ =rare earth metal) adopting monoclinic polymorphs in the paramagnetic state.

$R_5\text{Si}_x\text{Ge}_{4-x}$  alloys, and especially,  $\text{Gd}_5\text{Si}_x\text{Ge}_{4-x}$  compounds with  $x \leq \sim 2$  belong to an all important family of intermetallic materials, broadly investigated in the recent past due to coexistence of strong magnetocaloric, magnetostrictive, and magnetoresistive effects,<sup>9-13</sup> all of which are associated with magnetic phase transitions that occur simultaneously with martensiticlike structural transformations.<sup>8,11</sup> Of particular interest is one of the binary compounds— $\text{Gd}_5\text{Ge}_4$ . Like other members of the family, it has a distinctly layered crystal

structure (see Fig. 1) and exhibits strongly interconnected magnetic and crystallographic properties. At room temperature, PM  $\text{Gd}_5\text{Ge}_4$  adopts the  $\text{Sm}_5\text{Ge}_4$ -type structure [also known as the O(II)-type structure, Fig. 1(a)] which has no covalentlike Ge-Ge pairs between structurally identical two-dimensional slabs that are stacked along the  $b$  axis.<sup>14</sup> At  $T_N \cong 128$  K,  $\text{Gd}_5\text{Ge}_4$  orders antiferromagnetically (AFM) in a zero magnetic field,<sup>15-18</sup> retaining the same O(II) crystal structure as in the PM state. The AFM  $\text{Gd}_5\text{Ge}_4$  can be transformed into a nearly collinear FM state at low temperatures by applying a magnetic field exceeding  $\sim 10$  kOe. Simultaneously with the AFM  $\rightarrow$  FM transformation, the crystal structure changes over to the  $\text{Gd}_5\text{Si}_4$ -type structure [also

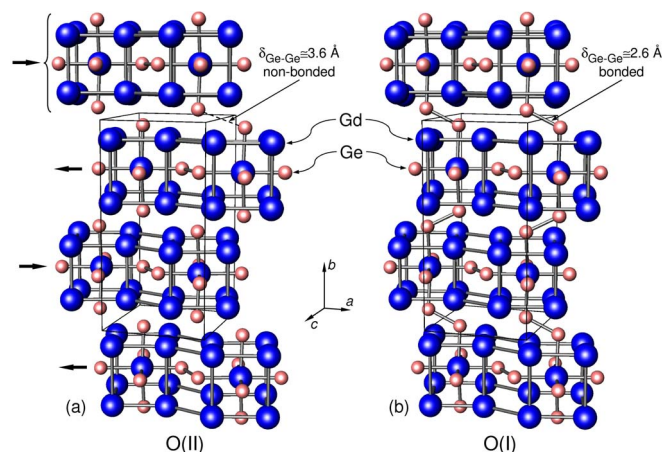


FIG. 1. (Color online) Perspective views of the crystal structures of  $\text{Gd}_5\text{Ge}_4$  in the paramagnetic and antiferromagnetic states (a) and in the ferromagnetic state (b). The bracket on the top left in (a) highlights a single slab. The numerical values indicate the interslab Ge-Ge distances in both structures. The arrows in (a) illustrate directions in which the slabs shear during the O(II) to O(I) transformation.

known as the O(I)-type structure,<sup>14</sup> Fig. 1(b)], in which the slabs remain practically identical to the O(II)-Gd<sub>5</sub>Ge<sub>4</sub> but their stacking is altered by shearing of the neighboring slabs in opposite directions along the *a* axis, and the interslab interactions become enhanced due to covalentlike interslab Ge-Ge bonds appearing as a result of the O(II) to O(I) polymorphic transition.<sup>19,20</sup> Hence, the O(I)-type polymorph is interslab bond rich, while the O(II)-type modification is interslab bond-poor structure.

This binary germanide is the only known member of the Gd<sub>5</sub>Si<sub>x</sub>Ge<sub>4-x</sub> family with an O(II)-AFM ground state despite a large positive Weiss temperature ( $\theta_p \cong 95$  K),<sup>16</sup> although there are preliminary indications that the ground state of this compound is indeed O(I)-FM Gd<sub>5</sub>Ge<sub>4</sub> which is not reached during a zero magnetic field cooling due to a kinetic arrest.<sup>21</sup> Furthermore, the anomalous behavior of the magnetic susceptibility of Gd<sub>5</sub>Ge<sub>4</sub> has been reported at temperatures as high as 230 K (approximately 100 K higher than  $T_N$ ), from which the beginning of some magnetic ordering process at 230 K has been hypothesized.<sup>22</sup> Based on high field ( $\sim 120$  kOe  $\leq H \leq 230$  kOe) magnetization measurements, the coexistence of short-range FM and AFM correlations due to breaking of the AFM ordering by a strong magnetic field was recently postulated for Gd<sub>5</sub>Ge<sub>4</sub> and a few other Ge-rich Gd<sub>5</sub>Si<sub>x</sub>Ge<sub>4-x</sub> compounds.<sup>23</sup> High-resolution x-ray powder diffraction performed in a 35 kOe magnetic field revealed that at 6.1 K, only  $\sim 93\%$  mol of Gd<sub>5</sub>Ge<sub>4</sub> has been transformed from the O(II) phase to the O(I) polymorphic modification, but the magnetization reaches  $\sim 99\%$  of its saturation value,<sup>19,24</sup> suggesting that at least some of the O(II)-Gd<sub>5</sub>Ge<sub>4</sub> orders ferromagnetically without a structural change. All of this, points to much more complex and intriguing physics than a simple competition of magnetic exchange and thermal energies as temperature and magnetic field vary. Here, we show that short range FM correlations extend far into what was previously thought to be the PM state of O(II)-Gd<sub>5</sub>Ge<sub>4</sub> and argue that these FM correlations result in a dynamic GP-like FM clustering at temperatures over 100 K higher than the temperature at which the system develops a long range antiferromagnetic order.

## II. EXPERIMENTAL DETAILS

A single crystal of Gd<sub>5</sub>Ge<sub>4</sub> was grown using the tri-arc pulling technique.<sup>25</sup> An oriented cubelike single crystal specimen with dimensions  $0.9 \times 1.0 \times 1.0$  mm<sup>3</sup> was prepared with its faces normal to the principal crystallographic directions. Details about the preparation and crystallographic orientation can be found elsewhere.<sup>26</sup> A detailed microscopic examination of several single crystalline specimens from the same batch<sup>27</sup> showed no detectable impurities other than  $\sim 1$  vol. % of Gd<sub>5</sub>Ge<sub>3</sub> present as extremely thin platelets that form in the solid state and are uniformly dispersed in the Gd<sub>5</sub>Ge<sub>4</sub> matrix. The Gd<sub>5</sub>Ge<sub>3</sub> compound orders antiferromagnetically  $\sim 50$  K below  $T_N$  of Gd<sub>5</sub>Ge<sub>4</sub>, and therefore, its presence in such a low concentration should have a negligible effect on bulk magnetism of the matrix. The dc magnetization and ac magnetic susceptibility were measured using a superconducting quantum interference device (SQUID) mag-

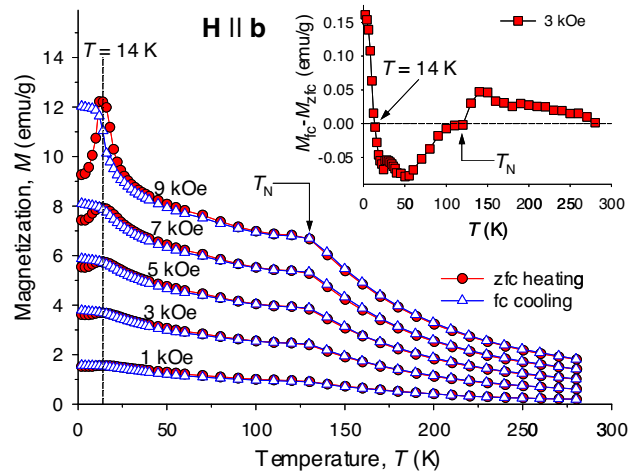


FIG. 2. (Color online) The magnetization of single crystal Gd<sub>5</sub>Ge<sub>4</sub> measured as a function of temperature between 1 and 9 kOe with the magnetic field vector parallel to the *b* axis. Inset shows the difference between the fc cooling and zfc heating magnetizations for a 3 kOe magnetic field.

netometer, MPMS-XL from Quantum Design, Inc. The ac magnetic susceptibility measurements were performed in a 10 Oe bias dc field with a 5 Oe ac drive field at a 125 Hz frequency. Before each measurement, the sample was zero-field cooled (zfc) from the paramagnetic state at 300 K to the desired temperature. After reaching this temperature, the magnetic field was applied and then  $M(T)$  data were collected during heating (zfc, heating) immediately followed by cooling (field cooled, fc, cooling) and then heating (fc, heating) measurements. Magnetic relaxation measurements were performed by fc cooling the sample in a 50 Oe field to a desired temperature and measuring the magnetization as a function of time at constant temperature and field immediately after the temperature was stable, usually 5–7 min after the target temperature was reached. We estimate that misalignment between the crystallographic axes and directions of both dc and ac magnetic field vectors did not exceed  $5^\circ$ .

## III. EXPERIMENTAL RESULTS

Figure 2 shows the magnetization of single crystal Gd<sub>5</sub>Ge<sub>4</sub> measured between 2 and 280 K in magnetic fields ranging from 1 to 9 kOe with the magnetic field vector parallel to the *b* axis. All  $M(T)$  curves exhibit anomalies at  $\sim 14$  K and  $\sim 128$  K, the latter corresponds to the Néel temperature,  $T_N$ . We note that because of the scale of Fig. 2, either of the irregularities for the 1 kOe  $M(T)$  data is difficult to see. Similar anomalies are also seen in  $M(T)$  data recorded with the magnetic field vector parallel to the *a* and *c* axes.<sup>26</sup> Below  $T_N$ , the magnetization along the *b* axis (and the *a* axis) increases with decreasing temperature, not following the behavior expected for a conventional AFM state in which the magnetization should remain constant below  $T_N$  (Ref. 28) when a magnetic field vector is perpendicular to the antiferromagnetic coupling axis (the Gd moments in O(II)-AFM Gd<sub>5</sub>Ge<sub>4</sub> are coupled along the *c* axis<sup>29,30</sup>). Below 14 K, the

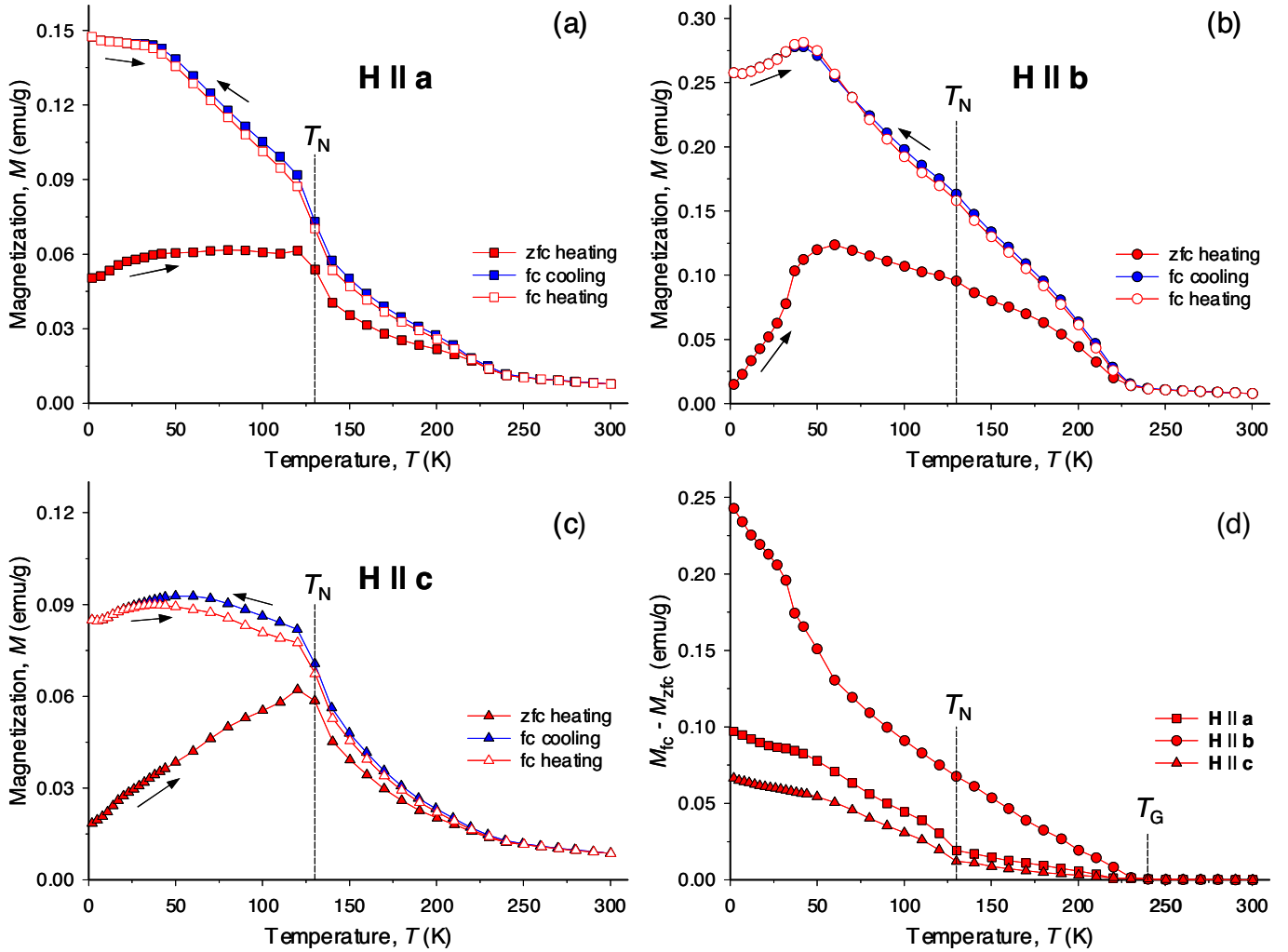


FIG. 3. (Color online) The magnetization of single crystal  $\text{Gd}_5\text{Ge}_4$  measured as a function of temperature in a 50 Oe magnetic field with the magnetic field vector parallel the  $a$  (a),  $b$  (b), and  $c$  axes (c). Panel (d) illustrates the difference between the fc cooling and zfc heating measurements. Néel temperature,  $T_N = 128$  K, is marked on every panel; panel (d) also indicates the common temperature ( $T_G$ ) at which the fc-zfc hysteresis sets in for all directions.

$M(T)$  anomaly originates from a small, field-dependent amount of O(I)-FM  $\text{Gd}_5\text{Ge}_4$  phase that precipitates in the O(II)-AFM matrix,<sup>16,21</sup> which is seen as a divergence of all fc cooling curves from the zfc heating curves, Fig. 2. Thermodynamically, the behavior developing with the increasing magnetic field in the vicinity of 14 K reveals a shifting balance between the thermal, magnetic, and strain energies, and the influence of strain on a kinetic arrest<sup>31</sup> that may occur in systems exhibiting magnetostructural phase transitions. The presence of low, field-dependent concentrations of the O(I)-FM  $\text{Gd}_5\text{Ge}_4$  is also supported by a weak hysteresis found in all  $M(T)$  curves between  $\sim 14$  K and  $T_N$ , where the fc cooling curves lie slightly below the zfc heating curves, as highlighted in the inset of Fig. 2. Increasing the field enhances both the magnitude of the kink at  $\sim 14$  K and the zfc-fc hysteresis below 14 K, thus signaling that the concentration of the O(I)-FM  $\text{Gd}_5\text{Ge}_4$  phase increases.

Figure 2 and its inset also indicate that above  $T_N$  the trend is reversed and fc cooling curves now exhibit a higher magnetization than the zfc heating curves, yet both remain closer

to one another than when compared in the AFM state. The deviation becomes progressively more and more evident as the temperature approaches  $T_N$ . Thus, weak FM correlations are also noticeable above  $T_N$ , i.e., they occur in the magnetically disordered state, which is quite unusual. The FM correlations above  $T_N$  are different from the O(I)-FM  $\text{Gd}_5\text{Ge}_4$  precipitating in the O(II)-AFM  $\text{Gd}_5\text{Ge}_4$  matrix below  $T_N$  because, as we show next, these high temperature FM correlations become enhanced in low magnetic fields, yet they are nearly completely suppressed in magnetic fields of 5 kOe and higher, which is just the opposite of the behavior<sup>16</sup> exhibited by the O(I)-FM precipitates of  $\text{Gd}_5\text{Ge}_4$ .

Figure 3 shows the  $M(T)$  behavior of single crystal  $\text{Gd}_5\text{Ge}_4$  measured with a 50 Oe magnetic field applied along the  $a$ ,  $b$  and  $c$  axes. The low temperature anomalies seen in Fig. 2 remain noticeable, but they now occur at various field direction-dependent temperatures ranging from 20 to 40 K. Unlike the higher field data where the magnetization behaviors along the  $a$  and  $b$  axes are quite similar to one other but both differ from that along the  $c$  axis,<sup>29,30</sup> all three of the



$M(T)$  curves are substantially different in a low magnetic field. Specifically, the  $b$ -axis magnetization is unusually large between 40 and 240 K, so that even the signature of the AFM ordering at  $T_N=128$  K becomes nearly unrecognizable, and both zfc and fc curves exhibit an FM-like transition around  $T_G=240$  K. Also, unlike the higher field ( $H \geq 1$  kOe) data of Fig. 2, where the difference between the zfc and fc magnetization changes sign at  $T_N$ , there is no sign change in the 50 Oe data. Furthermore, the 50 Oe fc cooling curves exhibit much higher magnetization than the zfc heating ones below  $T_G$ , and they also display a remarkable anisotropy [Figs. 3(a)–3(c)]. The unusually large zfc-fc hysteresis points to the presence of FM correlations in the PM state, which apparently sets at a much higher temperature than  $T_N$ . Comparing the behavior of  $M_{fc}-M_{zfc}$  with temperature in Fig. 3(d) to that in the higher field of Fig. 2 indicates that these low-field FM correlations extend into the AFM regime. With increasing field, however, FM correlations below  $T_N$  rapidly evolve into precipitates of O(I)-FM  $Gd_5Ge_4$ , which results in a smaller and differently behaving hysteresis (see inset of Fig. 2). Therefore, short-range FM correlations observed both in the PM and AFM states appear to be different from small precipitates of a long range FM  $Gd_5Ge_4$  which are manifested as a kink at  $T=14$  K in the zfc heating data. Short-range FM correlations are noticeable only in low fields and they are obviously enhanced along the  $b$  axis compared to the other two axes. They are also much enhanced in an fc process compared to the zfc heating process regardless of the geometrical relationship between the magnetic field vector and the crystallographic direction. We note here that in a polycrystalline sample of  $Gd_5Ge_4$ , an anomaly ascribed to FM correlations but without elaboration on their nature was observed below 225 K in  $M(T)$  data measured in a 500 Oe magnetic field.<sup>32</sup>

The FM correlations observed when  $T_N < T < T_G$  suggest anomalous behavior of the corresponding inverse magnetic susceptibility ( $H/M$ ), which is illustrated in Fig. 4. The 5 kOe data follow Curie-Weiss law above  $\sim 170$  K for all the three axes with a common paramagnetic Curie temperature,  $\theta_p=100$  K, and a practically equal effective magnetic moment of  $7.89 \mu_B/\text{Gd}$  atom, which is close to  $7.94 \mu_B$  expected for a free  $Gd^{3+}$  ion. The low field  $H/M$  curves, however, follow the Curie-Weiss law only above  $\sim 240$  K, exhibiting a rapid downturn below this temperature. Regardless of the geometrical relationship between the magnetic field vector and the crystallographic direction, the lower the field, the larger the negative deviation from a conventional PM behavior. The magnetic susceptibility along the  $b$  axis always exhibits a greater deviation below 240 K followed by the  $a$  then  $c$  axes in both zfc heating and fc cooling and fc heating curves indicating that the  $b$  axis plays a major role in defining short-range FM correlations. This observation correlates well with the fact that the magnetic field-induced FM state of  $Gd_5Ge_4$  is most stable when the field is applied along the  $b$ -axis axis, which also is the easy magnetization direction of the O(I)-FM  $Gd_5Ge_4$  (Ref. 26). Hence, magnetic anisotropy seen in Fig. 3 is consistent with FM clustering, which is controlled by the crystallographic anisotropy of this distinctly layered structure, and it is apparent that the  $b$ -axis

component of the magnetization of these clusters is dominant.

Magnetic anomalies between  $T_N$  and  $T_G$  are also manifested in the ac magnetic susceptibility, as shown in Fig. 5 for the  $b$  axis. The Curie-Weiss fit in the PM state above 240 K yields  $\theta_p=100$  K and  $p_{\text{eff}}=7.84 \mu_B/\text{Gd}$  atom, both values are nearly identical to those obtained from the dc  $M(T)$  data. Below  $\sim 240$  K, both the zfc heating and fc cooling  $1/\chi'(T)$  curves exhibit a large negative deviation from the paramagnetic behavior. Simultaneously, the nonzero values of the out-of-phase component of the ac magnetic susceptibility ( $\chi''$ ) indicate onset of an energy loss process, usually associated with domain dynamics, which is unexpected for a paramagnetic state but is consistent with a weak ferromagnetism, even though there is no onset of the long range magnetic order. The local minimum of  $1/\chi'(T)$  and the peak of  $\chi''(T)$  at  $\sim 210$  K correspond to the temperature at which the curvature of the  $\chi^{-1}(T)$  data is maximum [see Fig. 4(b)]. This also is the same temperature at which the  $\log(H/M)$  vs  $\log(T/T_C-1)$  curve shown in Fig. 4(d) (also see below) has a maximum slope. Unlike the dc magnetization data of Fig. 3, the ac magnetic susceptibility exhibits only a small zfc-fc hysteresis, apparently related to differences between static (dc field) and dynamic (ac field) magnetization processes.

Summarizing experimental results presented above, we conclude that FM correlations are present in both the AFM and PM states of  $Gd_5Ge_4$  at all temperatures below  $T_G=240$  K. At the microscopic scale, they can be understood by extending a Griffiths-type model,<sup>1</sup> in which ferromagnetic clustering above  $T_C$  in a diluted Ising ferromagnet results from a nonzero probability of populating neighboring lattice sites with interacting spins. Consider the O(II) phase of  $Gd_5Ge_4$  [Fig. 1(a)], where below  $T_N$  the coupling between Gd moments which belong to a same slab is FM, whereas the coupling between the neighboring slabs is AFM.<sup>29,30</sup> As temperature increases, both the intraslab FM and interslab AFM coupling weakens, and above  $T_N$ , the long range magnetic order disappears which normally should result in the PM state of the compound. We recall, however, that the slabs in O(II)  $Gd_5Ge_4$  have essentially the same structure as the slabs in any other  $Gd_5Si_xGe_{4-x}$  compound, including those adopting the interslab bond-rich O(I)-type structure in the PM state. The ground state of the O(I)-type phase [Fig. 1(b)] is FM, meaning that both the intraslab and interslab exchange interactions are ferromagnetic. On one hand, this enables us to postulate a possibility of random FM fluctuations which are due to interactions between neighboring FM ordered slabs. Considering that O(II)  $Gd_5Ge_4$  may order ferromagnetically without a structural change,<sup>19,20</sup> randomly occurring FM clustering of the ferromagnetically ordered slabs in the long range ordered O(II)-AFM  $Gd_5Ge_4$  matrix is quite feasible. On the other hand, it is well known that  $T_C$  of any O(I)- $Gd_5Si_xGe_{4-x}$  compound is always (and considerably) higher compared to a  $T_C$  of an interslab bond-deficient monoclinic<sup>8,14</sup> or O(II) polymorphic modifications with the same stoichiometry.<sup>33</sup> Hence, random FM interactions and clustering are likely to occur inside the magnetically disordered  $Gd_5Ge_4$  slabs at temperatures much higher than  $T_N$ . In this model, the FM fluctuations below  $T_N$  should be pseudo-

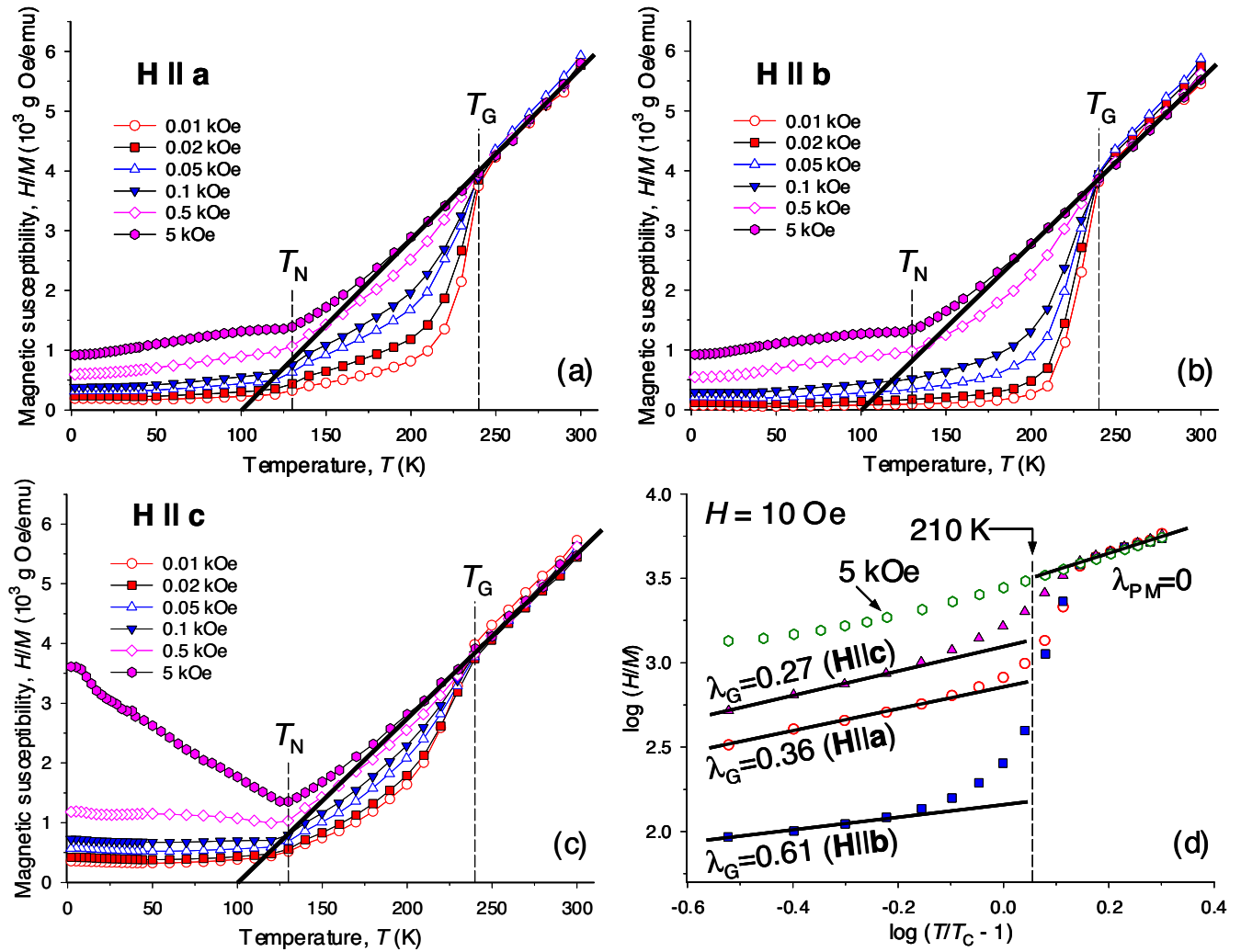


FIG. 4. (Color online) The fc cooling inverse dc magnetic susceptibility of single crystal  $\text{Gd}_5\text{Ge}_4$  measured along the  $a$  (a),  $b$  (b), and  $c$  axes (c) in magnetic fields ranging from 0.01 to 5 kOe. Panel (d) illustrates  $\log(H/M)$  vs  $\log(T/T_C - 1)$  for the three axes measured in a 10 Oe magnetic field and the same for the 5 kOe data along the  $b$  axis. Thick solid lines in (a)–(c) represent Curie-Weiss fits of the 5 kOe data. Solid lines in (d) are linear fits of  $\log(H/M)$  vs  $\log(T/T_C - 1)$  to establish  $\lambda$  in  $\chi(T) \propto (T - T_C)^{-(1-\lambda)}$ , with the dashed vertical line indicating the maximum slope of the curve for  $H \parallel b$ .

one-dimensional because they propagate along the  $b$  axis creating random FM clusters of FM ordered slabs, while these fluctuations and clustering are pseudo-two-dimensional, occurring predominantly in the  $ac$  plane and forming FM clusters inside the magnetically disordered slabs between  $T_N$  and  $T_G$ .

Anomalies of magnetization similar to those described above were recently reported in the low-field magnetization of polycrystalline  $\text{Tb}_5\text{Si}_2\text{Ge}_2$  (Ref. 7). These were correlated with the nanometer-scale O(I)-FM GP-type clusters detected in the monoclinic-PM  $\text{Tb}_5\text{Si}_2\text{Ge}_2$  by small angle neutron scattering experiments. The GP-like cluster onset temperature  $T_G \approx 200$  K was found to be consistent with the Curie temperatures of Si-rich O(I)-PM  $\text{Tb}_5\text{Si}_x\text{Ge}_{4-x}$  compounds where  $2.6 \leq x \leq 4$ . Extrapolation led to the expected magnetic ordering temperature of  $\sim 200$  K for a hypothetical O(I)-PM  $\text{Tb}_5\text{Si}_2\text{Ge}_2$  (Ref. 7). Similar to the behavior for  $\text{Tb}_5\text{Si}_2\text{Ge}_2$ , an “ordering” temperature of  $\sim 250$  K (which is quite close to the experimentally observed  $T_G = 240$  K) can

be obtained for “O(I)  $\text{Gd}_5\text{Ge}_4$ ” ( $x=0$ ) by extrapolating Curie temperatures of Si-rich O(I)-PM  $\text{Gd}_5\text{Si}_x\text{Ge}_{4-x}$  compounds where  $2 \leq x \leq 4$  (Ref. 14 and 34) (see inset of Fig. 6). With other similarities between the two systems, including the relationships between the crystal structure and magnetic behaviors, it is easy to accept that the FM correlations observed below  $\sim 240$  K in  $\text{Gd}_5\text{Ge}_4$  are related to a GP-like  $\text{Gd}_5\text{Ge}_4$  with  $T_G = 240$  K.

Further confirmation of this hypothesis may be obtained by analyzing magnetic susceptibility, which for a Griffiths phase, should be characterized by an exponent less than unity, that is,  $\chi(T) \propto (T - T_C)^{-(1-\lambda)}$ , where  $0 \leq \lambda < 1$  (Ref. 35). The large and positive value of the Weiss temperature indicates that the FM intraslab interactions are dominant compared to the AFM interslab interactions. Therefore, taking  $\theta_p = 100$  K as the ordering temperature ( $T_C$ ), we find that  $\lambda_G$  is highly anisotropic, varying from 0.27 ( $c$  axis) to 0.61 ( $b$  axis) for  $T_N < T < 170$  K, see Fig. 4(d). It becomes isotropic and zero, in the paramagnetic state, i.e.,  $\lambda_{\text{PM}} \equiv 0$  for  $T$

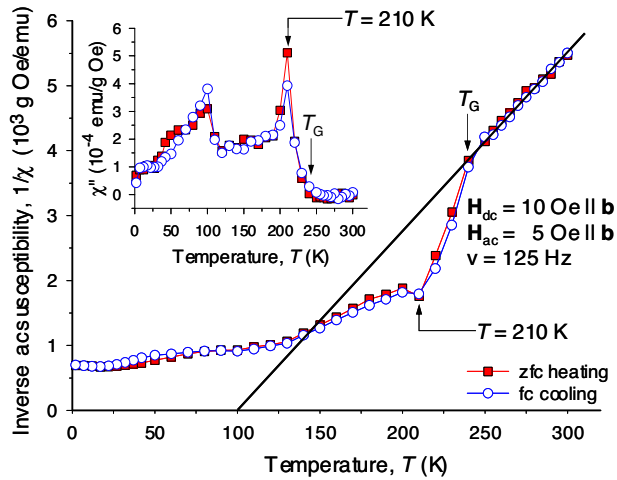


FIG. 5. (Color online) Temperature dependencies of the inverse ac magnetic susceptibility of single crystal  $Gd_5Ge_4$  ( $1/\chi'$ ) measured along the  $b$  axis with a bias dc field of 10 Oe applied along the same axis. The inset shows the out-of-phase component ( $\chi''$ ) of the ac susceptibility. The thick solid line is the Curie-Weiss fit.

> 240 K, as shown for the 10 Oe data in Fig. 4(d). The GP-like  $Gd_5Ge_4$  fully develops between  $\sim 180$  and 240 K, exhibiting a singularity around 210 K, which is indicated by the vertical line in Fig. 4(d). The same temperature for the Griffiths singularity is obtained for other low magnetic field  $M(T)$  data,  $H \leq 0.1$  kOe. When the field is increased,  $H > 0.1$  kOe, the size and/or concentration of the FM clusters is gradually reduced and GP  $Gd_5Ge_4$  becomes less and less distinguishable from the PM matrix, which under the influence of the magnetic field also develops a “preferred” magnetization direction coinciding with the magnetic field vector. When the field reaches 5 kOe, the Griffiths’s singularity

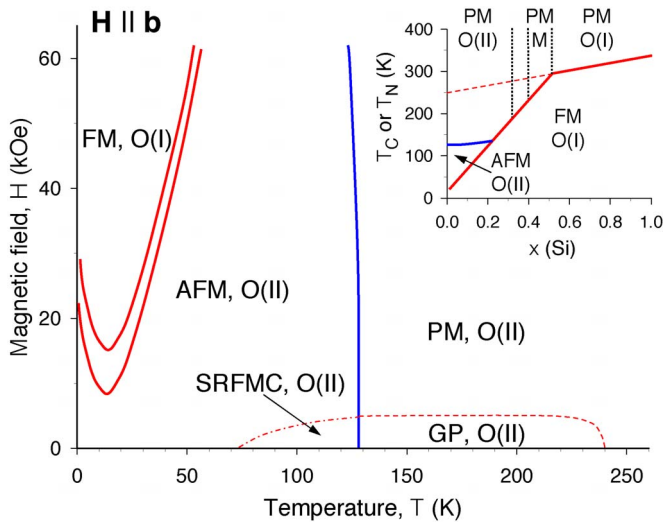


FIG. 6. (Color online) The refined  $H$ - $T$  magnetic phase diagram of  $Gd_5Ge_4$  single crystal for the initial magnetization with the magnetic field vector parallel to the  $b$  axis. The inset shows the extrapolation of the Curie temperature of the Si-rich O(I)-type  $Gd_5(Si_xGe_{1-x})_4$  (Ref. 14 and 34).

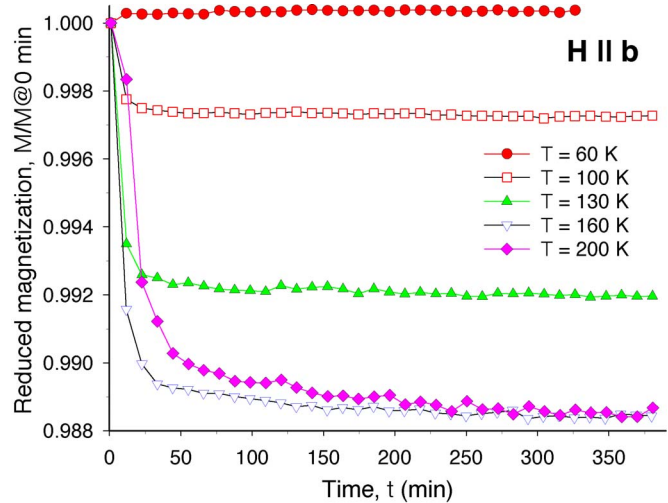


FIG. 7. (Color online) Time evolution of the magnetization of single crystal  $Gd_5Ge_4$  measured in a 50 Oe magnetic field applied parallel to the  $b$  axis after fc cooling the sample from 300 K to the temperature of the measurement.

disappears [Fig. 4(d)] and GP-like behavior of  $Gd_5Ge_4$  is completely suppressed.

We now consider macroscopic features that may be related to the development of the GP-like  $Gd_5Ge_4$ . Unlike in  $Tb_5Si_2Ge_2$ , where numerous stacking faults between twin variants of the monoclinic structure were considered an important factor in the formation of the Griffiths phase,<sup>7</sup> twins, and therefore, twin boundaries are absent in the orthorhombic  $Gd_5Ge_4$ . Therefore, the macroscopic mechanism responsible for a rapid development of FM clusters in  $Gd_5Ge_4$  must be different from what has been suggested for  $Tb_5Si_2Ge_2$ . A recent microstructural study of several  $R_5Si_xGe_{4-x}$  compositions, including  $Gd_5Ge_4$ , reveals the existence of ubiquitous microscopic features, seen as very thin plates with apparently  $Gd_5Si_xGe_{3-x}$  stoichiometry scattered through the bulk of all samples.<sup>36</sup> Noting that in  $Gd_5Ge_4$ , these plates should be the silicon-free  $Gd_5Ge_3$  binary phase and that the AFM ordering temperature of  $Gd_5Ge_3$  is 76 K (Ref. 37), it is safe to conclude that anomalies observed at and below  $T_G = 240$  K are not directly related to the intrinsic magnetism of the  $Gd_5Ge_3$  platelets, especially after recalling that these platelets make no more than 1–2 % of the total volume.<sup>19,20,25,36</sup> Since the formation of these plates appears to be related to a displacive-diffusional transformation occurring in the solid state during cooling, they form complex matrix-plate interfaces consisting of terraces that extend over many unit cell dimensions and risers that are considerably shorter. The terraces have a low mobility, whereas the risers have a high mobility, thus helping to quench in disorder at the interfaces. These disordered volumes facilitate atomic attachment and detachment, enabling the risers to produce transformation dislocations in the matrix. In turn, these dislocations serve as nucleation centers explaining the ease with which FM clusters emerge at high temperatures, in the GP-like regime.

The anomalous magnetic behavior below  $T_G$  is also clearly seen from the magnetic relaxation data illustrated in Fig. 7. Here, the single crystal was field cooled ( $H = 50$  Oe at



a rate 10 K/min) from 300 K to the temperature of the measurement and then the magnetization was measured every 10 min over the next 5.5 to 6.5 h. Between  $T_N$  and  $T_G$ , the isofield and isothermal magnetization falls off by about 1% within the first 20–30 min and then exhibits a tendency towards saturation, while still decaying slowly. This reduction of the magnetization with time is quite unusual since normally magnetization relaxes in the opposite way, i.e., it increases with time at constant magnetic field and temperature. Furthermore, the curves depicted in Fig. 7 are not exponential functions of time, and therefore, magnetization decays appear to be unrelated to any thermally activated process. Reduction of the magnetization with time correlates well with the observed zfc-fc hysteresis illustrated in Fig. 3(d), showing that a constant magnetic field reduces FM-like coupling when the sample is kept in the field for a long enough time. This serves as an additional proof that the magnetic field suppresses FM fluctuations and clustering, in the GP-like regime. As expected, above  $T_G$  (not shown in Fig. 7) and well below  $T_N$  (Fig. 7,  $T=60$  K) the magnetization of  $Gd_5Ge_4$  remains constant with time. A small initial decrease of the magnetization at 100 K, when the system is already in the AFM state but the temperature remains close to  $T_N$  also supports our suggestion (see above) that dynamic, short range FM correlations occur in a low magnetic field even in the antiferromagnetically ordered  $Gd_5Ge_4$ .

The updated  $H$ - $T$  phase diagram of  $Gd_5Ge_4$  (assuming zfc cooled sample and first magnetic field application) including the presence of the GP-like regime above  $T_N$  is depicted in Fig. 6 for the magnetic field vector parallel to the  $b$  axis (see Ref. 26 for the diagrams along the other two axes, which however, do not include the Griffiths phase region). Even though the low-field, short-range FM correlations extend into the AFM regime, they are microscopically inequivalent to those that occur above the  $T_N$ . We, thus, designate this phase region as short-range ferromagnetic clustering (SRFMC). It appears that just like in the Griffiths phase region, clustering in the SRFMC phase region is dynamic, which is possible because it does not involve crystallographic phase change, and therefore, is not hindered by the related strain.

#### IV. CONCLUSIONS

As follows from the low-field magnetic properties of a single crystal of  $Gd_5Ge_4$ , the system exhibits complex interplay between long range and short-range magnetic order. In addition to a small fraction of a static FM component (concentration of which steadily increases with the increasing magnetic field between 0 and  $\sim 9$  kOe) present in the AFM matrix below  $\sim 14$  K, dynamic short-range ferromagnetic clustering is observed between 70–80 K and  $T_N$ . While the static FM component adopts the O(I)-type structure, we believe that the dynamic FM clusters maintain the O(II)-type crystal structure, which is the same as for the AFM matrix. Above  $T_N=128$  K but below  $T_G=240$  K, a different type of short-range ferromagnetic correlations and dynamic FM clustering, which may be attributed to the Griffiths phaselike state of  $Gd_5Ge_4$ , is also observed. Unlike the negligible anisotropy of the true paramagnetic state above 240 K, the Griffiths phaselike  $Gd_5Ge_4$  exhibits strong magnetic anisotropy with the  $b$  axis being clearly the direction with the largest magnetization. The latter is consistent with the same axis being the easy magnetization direction of the long range ordered FM  $Gd_5Ge_4$  phase. Signatures of the short-range ferromagnetic correlations are easily suppressed by magnetic fields exceeding  $\sim 5$  kOe. Microscopically, the formation of the Griffiths-like phase can be related to the competition of the interslab and intraslab magnetic exchange interactions that are present in a distinctly layered crystal structure of the compound. Macroscopically, the appearance of the Griffiths-like phase may be enhanced by the precipitates of thin plates of  $Gd_5Ge_3$  present in the sample.

#### ACKNOWLEDGMENTS

The Ames Laboratory is operated for the U.S. Department of Energy by Iowa State University under Contract No. W-7405-ENG-82. This work was supported by the Office of Basic Energy Sciences, Materials Sciences Division of the U.S. Department of Energy.

\*Corresponding author. Electronic address: vitkp@ameslab.gov

<sup>1</sup>R. B. Griffiths, Phys. Rev. Lett. **23**, 17 (1969).

<sup>2</sup>M. B. Salamon, P. Lin, and S. H. Chun, Phys. Rev. Lett. **88**, 197203 (2002).

<sup>3</sup>J. Deisenhofer, D. Braak, H.-A. Krug von Nidda, J. Hemberger, R. M. Eremina, V. A. Ivanshin, A. M. Balbashov, G. Jug, A. Loidl, T. Kimura, and Y. Tokura, Phys. Rev. Lett. **95**, 257202 (2005).

<sup>4</sup>M. C. de Andrade, R. Chau, R. P. Dickey, N. R. Dille, E. J. Freeman, D. A. Gajewski, M. B. Maple, R. Movshovich, A. H. Castro Neto, G. Castilla, and B. A. Jones, Phys. Rev. Lett. **81**, 5620 (1998).

<sup>5</sup>H. Deguchi, M. Aikawa, K. Ohtani, and S. Takagi, J. Magn. Mater. **177-181**, 87 (1998).

<sup>6</sup>M. Suzuki, I. S. Suzuki, T. M. Onyango, and T. Enoki, J. Phys.

Soc. Jpn. **73**, 206 (2004).

<sup>7</sup>C. Magen, P. A. Algarabel, L. Morellon, J. P. Araújo, C. Ritter, M. R. Ibarra, A. M. Pereira, and J. B. Sousa, Phys. Rev. Lett. **96**, 167201 (2006).

<sup>8</sup>W. Choe, V. K. Pecharsky, A. O. Pecharsky, K. A. Gschneidner, Jr., V. G. Young, Jr., and G. J. Miller, Phys. Rev. Lett. **84**, 4617 (2000).

<sup>9</sup>V. K. Pecharsky and K. A. Gschneidner, Jr., Phys. Rev. Lett. **78**, 4494 (1997).

<sup>10</sup>V. K. Pecharsky and K. A. Gschneidner, Jr., Appl. Phys. Lett. **70**, 3299 (1997).

<sup>11</sup>L. Morellon, P. A. Algarabel, M. R. Ibarra, J. Blasco, B. García-Landa, Z. Arnold, and F. Albertini, Phys. Rev. B **58**, R14721 (1998).

<sup>12</sup>L. Morellon, J. Stankiewicz, B. García-Landa, P. A. Algarabel,

- and M. R. Ibarra, *Appl. Phys. Lett.* **73**, 3462 (1998).
- <sup>13</sup>E. M. Levin, V. K. Pecharsky, and K. A. Gschneidner, Jr., *Phys. Rev. B* **60**, 7993 (1999).
- <sup>14</sup>V. K. Pecharsky and K. A. Gschneidner, Jr., *J. Alloys Compd.* **260**, 98 (1997).
- <sup>15</sup>E. M. Levin, V. K. Pecharsky, K. A. Gschneidner, Jr., and G. J. Miller, *Phys. Rev. B* **64**, 235103 (2001).
- <sup>16</sup>E. M. Levin, K. A. Gschneidner, Jr., and V. K. Pecharsky, *Phys. Rev. B* **65**, 214427 (2002).
- <sup>17</sup>C. Magen, L. Morellon, P. A. Algarabel, C. Marquina, and M. R. Ibarra, *J. Phys.: Condens. Matter* **15**, 2389 (2003).
- <sup>18</sup>F. Casanova, A. Labarta, X. Batlle, J. Marcos, L. Mañosa, A. Planes, and S. de Brion, *Phys. Rev. B* **69**, 104416 (2004).
- <sup>19</sup>V. K. Pecharsky, A. P. Holm, K. A. Gschneidner, Jr., and R. Rink, *Phys. Rev. Lett.* **91**, 197204 (2003).
- <sup>20</sup>Y. Mudryk, A. P. Holm, K. A. Gschneidner, Jr., and V. K. Pecharsky, *Phys. Rev. B* **72**, 064442 (2005).
- <sup>21</sup>S. B. Roy, M. K. Chattopadhyay, P. Chaddah, J. D. Moore, G. K. Perkins, L. F. Cohen, K. A. Gschneidner, Jr., and V. K. Pecharsky, *Phys. Rev. B* **74**, 012403 (2006).
- <sup>22</sup>J. Szade and G. Skorek, *J. Magn. Magn. Mater.* **196-197**, 699 (1999).
- <sup>23</sup>F. Casanova, S. de Brion, A. Labarta, and X. Batlle, *J. Phys. D* **28**, 3343 (2005).
- <sup>24</sup>V. K. Pecharsky and K. A. Gschneidner, Jr., in *Magnetism and Structure in Functional Materials*, edited by A. Planes, L. Mañosa, and A. Saxena (Springer, Berlin, 2005), p. 199.
- <sup>25</sup>D. L. Schlagel, T. A. Lograsso, A. O. Pecharsky, and J. A. Sampaio, in *Light Metals 2005*, edited by H. Kvande (The Minerals, Metals and Materials Society, TMS, Warrendale, PA, 2005), p. 1177.
- <sup>26</sup>Z. W. Ouyang, V. K. Pecharsky, K. A. Gschneidner, Jr., D. L. Schlagel, and T. A. Lograsso, *Phys. Rev. B* **74**, 024401 (2006).
- <sup>27</sup>O. Ugurlu, Ph.D. thesis, Iowa State University, 2006.
- <sup>28</sup>L. Néel, *Ann. Phys.* **5**, 232 (1936).
- <sup>29</sup>E. M. Levin, K. A. Gschneidner, Jr., T. A. Lograsso, D. L. Schlagel, and V. K. Pecharsky, *Phys. Rev. B* **69**, 144428 (2004).
- <sup>30</sup>L. Tan, A. Kreyssig, J. W. Kim, A. I. Goldman, R. J. McQueeney, D. Wermeille, B. Sieve, T. A. Lograsso, D. L. Schlagel, S. L. Budko, V. K. Pecharsky, and K. A. Gschneidner, Jr., *Phys. Rev. B* **71**, 214408 (2005).
- <sup>31</sup>P. Chaddah, A. Banerjee, and S. B. Roy, cond-mat/0601095 (unpublished).
- <sup>32</sup>M. K. Chattopadhyay, M. A. Manekar, A. O. Pecharsky, V. K. Pecharsky, K. A. Gschneidner, Jr., J. Moore, G. K. Perkins, Y. V. Bugoslavsky, S. B. Roy, P. Chaddah, and L. F. Cohen (unpublished).
- <sup>33</sup>V. K. Pecharsky, G. D. Samolyuk, V. P. Antropov, A. O. Pecharsky, V. K. Pecharsky, and K. A. Gschneidner, Jr., *J. Solid State Chem.* **171**, 57 (2003).
- <sup>34</sup>A. O. Pecharsky, K. A. Gschneidner, Jr., V. K. Pecharsky, and C. E. Schindler, *J. Alloys Compd.* **338**, 126 (2002).
- <sup>35</sup>A. H. Castro Neto, G. Castilla, and B. A. Jones, *Phys. Rev. Lett.* **81**, 3531 (1998).
- <sup>36</sup>O. Ugurlu, L. S. Chumbley, D. L. Schlagel, and T. A. Lograsso, *Acta Mater.* **54**, 1211 (2006).
- <sup>37</sup>T. Tsutaoka, Y. Nishiume, and T. Tokunaga, *J. Magn. Magn. Mater.* **272-276**, E421 (2004).